

Supporting Information

Photoarchitectonic Hydrogels for Synergistic *In Vitro* Chemo- Phototherapy of Breast Cancer

Shatabdi Paul,^{a,b} Binduma Yadav,^{b,c} Mahesh D Patil,^{a,‡} Anil Kumar Pujari,^{a,d} Umesh Singh,^a
Vikas Rishi,^c and Jayeeta Bhaumik^{a,b*}

^aCenter of Innovative and Applied Bioprocessing (CIAB),
Department of Nanomaterials and Application Technology,
Department of Biotechnology (DBT), Government of India,
Sector 81 (Knowledge City), S.A.S. Nagar 140306, Punjab, India

^bRegional Centre for Biotechnology,
Department of Biotechnology (DBT), Government of India,
Faridabad, Haryana 121001

^cNational Agri-Food Biotechnology Institute (NABI)
Department of Biotechnology (DBT), Government of India,
Sector 81 (Knowledge City), S.A.S. Nagar 140308, Punjab, India

^dDepartment of Chemical Sciences, Indian Institute of Science Education and Research,
Sector-81 (Knowledge City), S.A.S Nagar, 140306, Mohali, Punjab, India

[‡]Present address: Chemical Engineering & Process Development Division, CSIR-National
Chemical Laboratory, Dr. Homi Bhabha Road, Pune 411008, India

*Corresponding author's email: jayeeta@ciab.res.in, jbhaumi@gmail.com

Table of contents

S1. Chemical and Instruments.....	S3
S2. Experimental Section.....	S3
S3. Optimization of the preparation of CDs.....	S7
S4. Characterization of CDs	S8
S5. Loading of DOX on CDs.....	S9
S6. Optimization of the concentrations of ZnPc, PEGMA, PAA.....	S13
S7. Swelling index of the ZnPc-PP H.....	S13
S8. Brunauer-Emmett-Teller (BET) analysis.....	S15
S9. Singlet oxygen quantification assay of the DOX@CDs-ZnPc-PP H.....	S19
S10. Optimization of laser light intensity for anticancer activity.....	S20
S11. Combination index.....	S21
S12. References.....	S21

S1. Chemicals and Instruments

Materials. Lignin (kraft type), Zinc phthalocyanine (ZnPc), 3-(4,5-dimethylthiazol-2-yl)-2,5-diphenyltetrazolium bromide (MTT), dimethyl sulfoxide (DMSO) phosphate buffer saline (PBS) and 1,3-Diphenylisobenzofuran (DPBF), thiazolyl blue tetrazolium bromide, doxorubicin RNase A, neutral buffered formalin (NBF), Hoechst33342, propidium iodide (PI), and dichloro-dihydro-fluorescein-diacetate (DCFH-DA) were purchased from Sigma-Aldrich (USA). Pluronic[®] F-68 (PF-68) stabilizer was purchased from Himedia laboratories (Mumbai, India). Acetone (99.9%, Merck, Germany) was used to prepare the organic and lipid phase in the preparation of nanoparticles. HPLC grade methanol, ethyl acetate, and acetonitrile were obtained from Merck (Germany). Waters UPLC system (Waters, USA) controlled by Empower[™] pro software, equipped with an autosampler and analytical C18 column (eclipse C18 column, 4.6 mm × 100, 5 μ m). Dulbecco's modified eagle media (DMEM), and fetal bovine serum (FBS) were procured from (Gibco, USA).

S2. Experimental section

Characterizations of CDs, DOX, and DOX@CDs. The morphology of the CDs was evaluated using HR-TEM analysis. Further, UV-Vis absorption spectra of CDs solution were measured in the range of 200–700 nm by using a UV-vis absorbance spectrometer (Shimadzu 2600). The size and surface charge of CDs were assessed using a Malvern zetasizer. The FT-IR [Fourier transform infrared (Agilent, model Cary 600 series)] spectroscopy was carried out to determine the characteristics peak present in CDs by FT-IR spectrometer (Agilent, model Cary 600 series) within the spectral window in the range of 500-4000 cm^{-1} . Further, the crystallinity of the material was found by powered X-Ray Diffraction (XRD) (Rigaku Smartlab SE model).

Characterization of Hydrogels. Transmission electron microscopy (TEM, JEM-2100F) was used to examine the morphologies of several HMSNs. The Malvern Zetasizer NanoZS was

used to measure the zeta potential of ZnPc-PP H and DOX@CDs loaded ZnPc-PEGMA/PAA hydrogels. Further, the successful establishment of ZnPc-PP H was successfully established supported by using ultraviolet-visible (UV-vis) spectroscopy. The transmittance of hydrogel was also determined and validated by ultraviolet-visible (UV-vis) spectroscopy. The high powder X-ray diffraction was measured from 10-70 degrees using an X-ray diffractometer with a rotating anode 200B/D/MAX-RB (XRD). Later, Fourier transforms infrared spectroscopy analysis was performed to determine the alterations in chemical functional groups on the surface of the ZnPc-PP H surface using an infrared spectrophotometer. Afterward, Quantachrome Autosorb IQ was used for BET analysis (Germany) to calculate the specific surface area and pore size features of ZnPc-PP H and DOX@CDs loaded ZnPcPP H. The standard process is as follows: in a quartz tube, 50 mg of probes were placed, and it was preheated for 110 min at 500 °C with He flowing through it at 50 mL/min before being cooled to 150 °C. Following the removal of the physisorbed NH₃ under He flows for 230 minutes, the sample was adsorbed with 1% NH₃/He (50 mL/min) for 30 min at the same temperature. Desorption was measured between 150 and 700 °C at 10 °C/min as He flowed through the system (50 mL/min).

Rheological studies. The rheological properties of the samples were determined using an MCR-101 rheometer (Anton Paar, Japan) with a parallel plate at a temperature of 37 °C. Throughout all experiments, a 0.5 mm gap was maintained between the plate and hydrogel samples. To avoid water evaporation during the experiment, liquid paraffin was applied to the plates. Before testing, the hydrogels were incubated for 1 h. The linear viscoelastic range (LVE) of the hydrogels was determined using an amplitude sweep test. After that, the hydrogels were subjected to a varying amplitude of strain (high 100% and low 1%), and changes in the storage modulus values were recorded to assess the mechanical property of the hydrogels under strain. These hydrogels were also subjected to frequency sweep measurements with a frequency range

of 0.01 to 100 rad/s at 1% amplitude. The viscosity and shear-thinning characteristics of ZnPc-PP H were investigated using a flow sweep experiment in the range 0.01-100 s⁻¹.

Swelling behavior of hydrogels. The swelling behavior of hydrogels was investigated at pH 7.4. For this, a known of the lyophilized ZnPc-PP H was immersed in PBS buffer solution (100 mL) at pH 7.4 for 85 h at 37 °C, until a consistent weight was achieved. Following that, at various time intervals (0, 1, 2, 3, 4, 5, 6, 12, 24, 36, 48, 72, 96 h), the hydrogels were removed from the solution at defined time intervals and gently wiped to remove surface-bound water before being weighed. The volume of the aqueous medium absorbed by the hydrogels was calculated gravimetrically using the following equation.¹

$$\text{Swelling ratio (\%)} = \frac{W_s - W_o}{W_o} \times 100 \quad \dots\dots\dots \text{(Eq. 2)}$$

where W_o and W_s are the initial and swollen weights of hydrogels, respectively, at time t.

pH responsiveness of the ZnPc-PP H. To examine the pH-responsive features of ZnPc-PP H, two distinct sections of the developed hydrogel of similar weight were cut. The dissected hydrogels were subsequently immersed in varying pH of PBS buffer solutions (5.5, 7.4). The mass of all hydrogel samples was then measured at varied time intervals at 25 °C.

In vitro pH-triggered drugs release. The drug release profile of DOX and ZnPc from the hydrogel was studied at various pH to demonstrate the pH sensitivity of the samples. For this, 2mg of hydrogel was accurately weighed and placed in dialysis bags (MWCO, 3.500 Da) and dispersed in 40 mL of PBS (pH 5.0). The release study was conducted at 37 °C with stirring (100 rpm). Accompanying at pre-determined time intervals, the 1 mL of released media was withdrawn and replaced with fresh 1 mL of PBS. Another, same set of experiments was conducted to monitor release behavior at pH 7.4. The collected release media was lyophilized, further, the lyophilized sample was injected in UPLC-PDA to estimate the released profile of

DOX and ZnPc, respectively. For this, UPLC analysis of DOX and ZnPc, lyophilized sample dissolved in the mixture of acetonitrile and water (3:7, v/v), subsequently injected in the UPLC autosampler as condition using Waters UPLC system [(Waters, USA) controlled by EmpowerTM pro software, equipped with an autosampler and analytical C18 column (eclipse C18 column, 4.6 mm × 100, 5 μm)]. DOX and ZnPc were eluted isocratically at a flow rate of 1 mL/min using acetonitrile: water (30:70) as eluent and detected using Waters 2998 PDA detector at the wavelength ranging from 200-800 nm, but the analysis was carried out at 490 nm and 665 nm, respectively at 30 °C. The release profile was replicated three times.

Detection of singlet oxygen quantum yield (SOQY). The singlet oxygen produced by DOX@CDs-ZnPc-PP H was detected by singlet oxygen was quantified using 1,3-diphenylisobenzofuran (DPBF)². As DPBF reacts with reactive oxygen species, its absorbance decreases, resulting in an accurate indicator of singlet oxygen generation (ROS). Briefly, in the DPBF photodegradation experiment, 1 mg/mL stock solutions of each probe namely, ZnPc, only was mixed with DPBF solution 1 mg/mL, in DMSO) respectively. The cuvette containing the above-mentioned probes and DPBF was irradiated at specific intervals with a 650 nm red laser with a net emitting power of 30 mW (or 3.52 x10¹⁸ photons/cm². s⁻¹, considering photons of wavelength 650 nm) after the absorbance spectrum was already recorded. The laser light is kept 1 cm away from the sample to be irradiated. To monitor the study, the standard (ZnPc is 0.67) was replaced by adding 2 μL of different probes (CDs, only DOX, DOX@CDs, ZnPc-P-P H, and DOX@CDs-ZnPc-PP H), and DPBF absorbance at 410 nm was monitored. The singlet oxygen quantum yield (Φ_Δ) of all the agents was determined to the decreasing slope of DPBF concentration using the following formula.^{3,4}

$$\Phi_{\Delta}(U) = \Phi_{\Delta}(St) \cdot S(U) / S(St) \quad \dots\dots\dots \text{(Eq. 3)}$$

Where, S(U) and S(St) represent the slope of an unknown and standard sample, respectively.

The decrease in the absorbance of DPBF was plotted against increasing time exposure of the laser at definite time intervals. and the obtained linear slopes were used to measure the singlet oxygen quantum yield (Φ_{Δ}). The reported standard value of the Φ_{Δ} value of ZnPc is 0.67. The Φ_{Δ} values of all the agents have been calculated using the above-mentioned equation.

S3. Optimization of the Preparation of CDs

The effects of reaction time, hydrothermal temperature, and additive concentration on the synthesis of CDs were established. For this, the preparation of CDs was conducted to determine the optimal factors using size, surface charge, and pH so that the developed CDs can easily internalize and interact with the tumor cells. **Figure S1** exhibits the initial settings of the synthesis process. Briefly, the effect of different ratios of lignin & folic acid (w/w percentage) was assessed using the size, surface charge, and pH. Further, the effect of temperatures ranging from 100 to 200 °C, respectively was evaluated. We observed that the optimum temperature (160 °C) was the most suitable for the synthesis of C dots, in which obtained the size is 110 nm. Next, the optimum time for the synthesis of C dots was optimized. The optimized parameters for the development of C dots were a 2:1 ratio of lignin to folic acid, a temperature of 160 °C, and a time of 8 h for higher C dot synthesis (47% yield). The optimized parameter obtained the CDs with an average size of 120 nm, a surface charge of -28 mV, and a pH of 6.98.

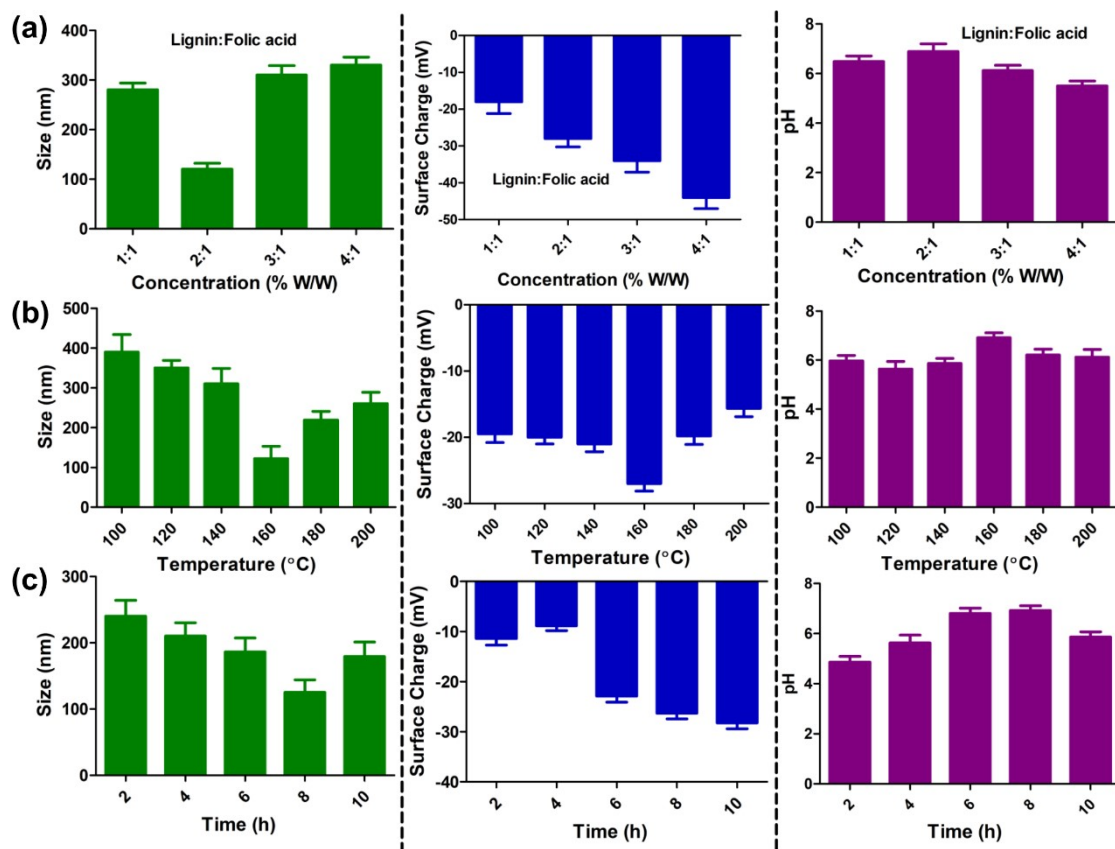


Figure S1. Effect of (a) Lignin: Folic acid ratio; (b) Temperature; (c) Time on the size, surface charge, and pH of the synthesized CDs.

S4. Characterization of CDs

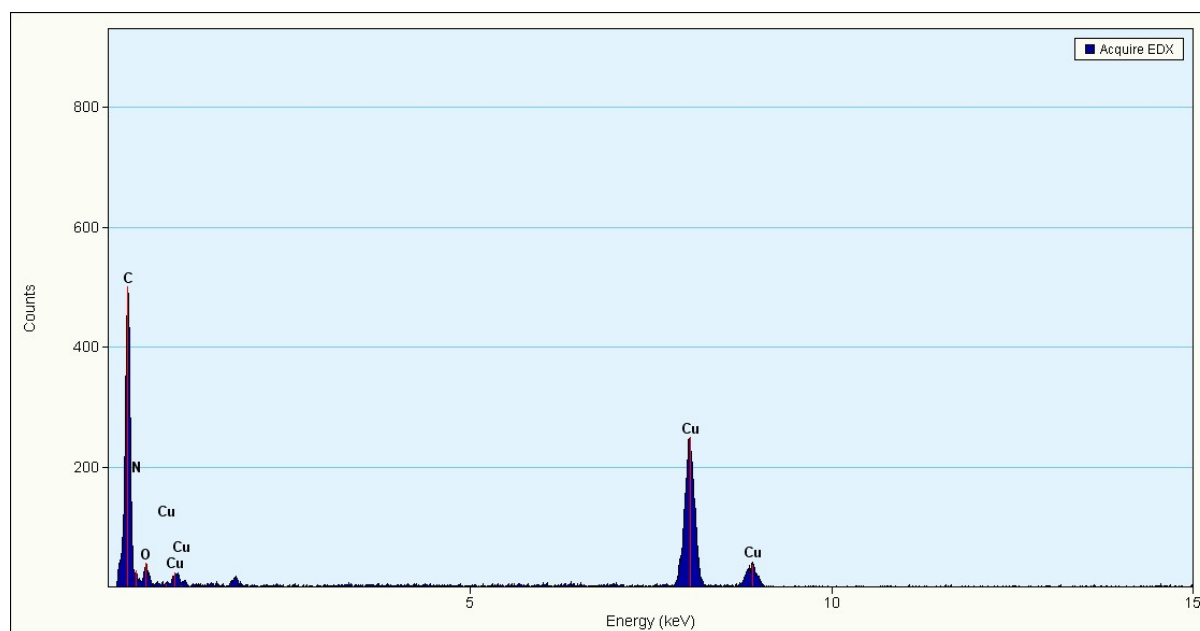


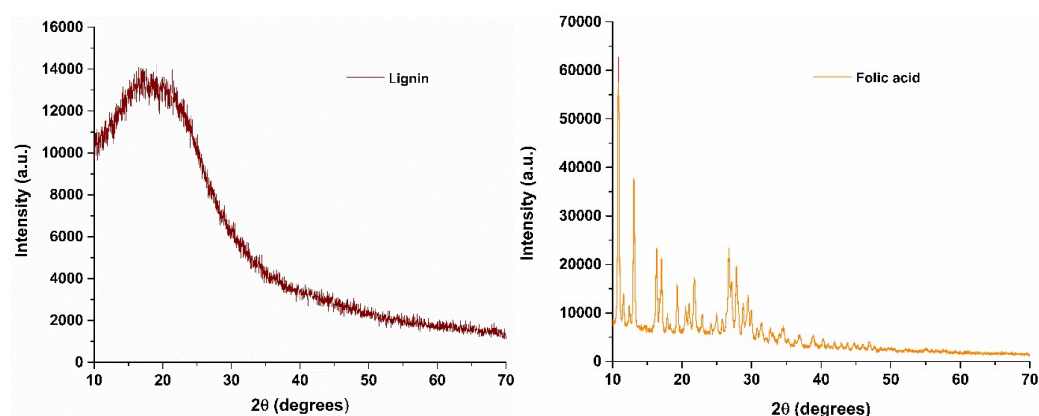
Figure S2. EDS spectrum of CDs.

Table S1. Elemental analysis of the developed CDs

S. No.	***Quantification		Results**				
	Correction method:	Thickness	*				
			Element	Weigh %	Atomic %	Uncert. %	Detector Correction
1	C(K)	94.00	94.99	1.78	0.26	4.00	1
2	N(K)	3.70	3.21	0.33	0.26	3.82	1
3	O(K)	2.00	1.78	0.22	0.49	2.00	1

The newly synthesized CDs absorption peak was observed at 280 nm ($n-\pi^*$ transitions) and 360 nm ($\pi-\pi^*$ transitions), respectively, which indicated the presence of Folic acid (Figure 1g).⁵ This perfect existence of these two bands in established CDs with folic acid confirms the successful attachment of folic acid.

XRD pattern of CDs

**Figure S3.** XRD spectra of lignin (left) and folic acid (right).

S5. Loading of DOX on CDs

For the coupling reaction, EDC and NHS were used in the conjugation of DOX with CDs. For this, CDs (10 mg/mL) and EDC (80 μ L, 5 mg/mL), and, NHS (80 μ L, 5 mg/mL) were

combined in a glass vial ⁶ DOX (1 mg/mL) was then added, the total reaction volume was maintained to 2 mL. PBS buffer was used to prepare all of the stock solutions as well as the final reaction mixture. Conjugation reactions were set up and stirred for 12 hours at 120 rpm. The c dots-drug conjugate solutions were centrifuged at 15000 rpm for 60 min at 4 °C once the reaction was finished. After two each colored supernatant, which contained unconjugated, was discarded until clear supernatants were seen from each reaction mixture. The resulting supernatants were then filtered through a nylon-66 membrane syringe filter and analyzed using Waters UPLC system (Waters, USA) controlled by EmpowerTM pro software, equipped with an autosampler and analytical C18 column (eclipse C18 column, 4.6 mm × 100, 5µm). DOX was eluted isocratically at a flow rate of 1 mL/min using acetonitrile: water (30:70) as eluent and detected using Waters 2998 PDA detector at the wavelength 490 nm, at 30 °C.

The percent conjugation of DOX onto the CDs was determined using the following equation (4).

$$\text{Loading \%} = [(\text{Total drug added} - \text{Drug in the supernatant})/(\text{Total drug added})]*100$$

$$\text{Loading \%} = 64$$

Table S2. Loading of DOX on the CDS

Parameters	DOX $y=10268x^a$, $R^2 = 0.9949$
AUC ^b	43762 ± 352
[Total drug] ^c (mg)	0.1
[drug in supernatant] ^d (mg)	0.004

^a Linear equation of DOX for quantitative determination using UPLC, ^b Area under the curve in the HPLC chromatogram of the supernatant solution containing DOX after centrifugation. ^c concentrations of DOX in the supernatant solution, calculated using linear regression equation $y = mx+c$. ^d total dox used to determine the percent of DOX conjugation on the CDs. This was calculated using the equation.

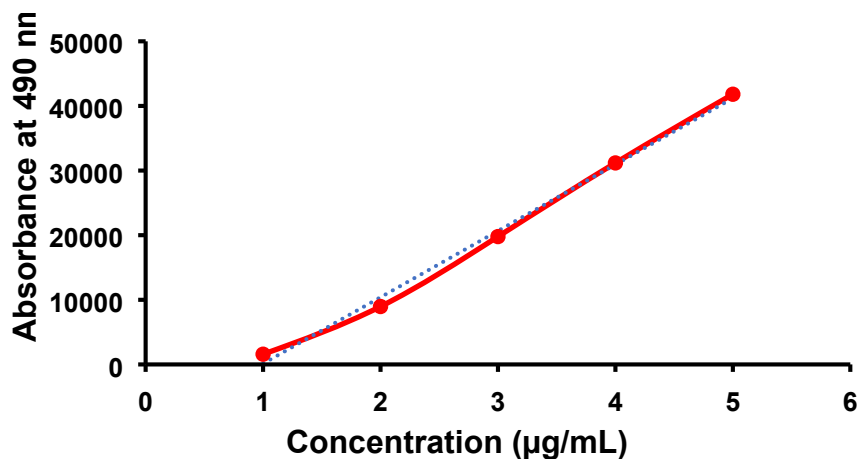


Figure S4. The standard plot of DOX using water as a solvent

x= 0.004 mg/ml

Total volume = 9 ml

0.036 mg dye released in 9 ml

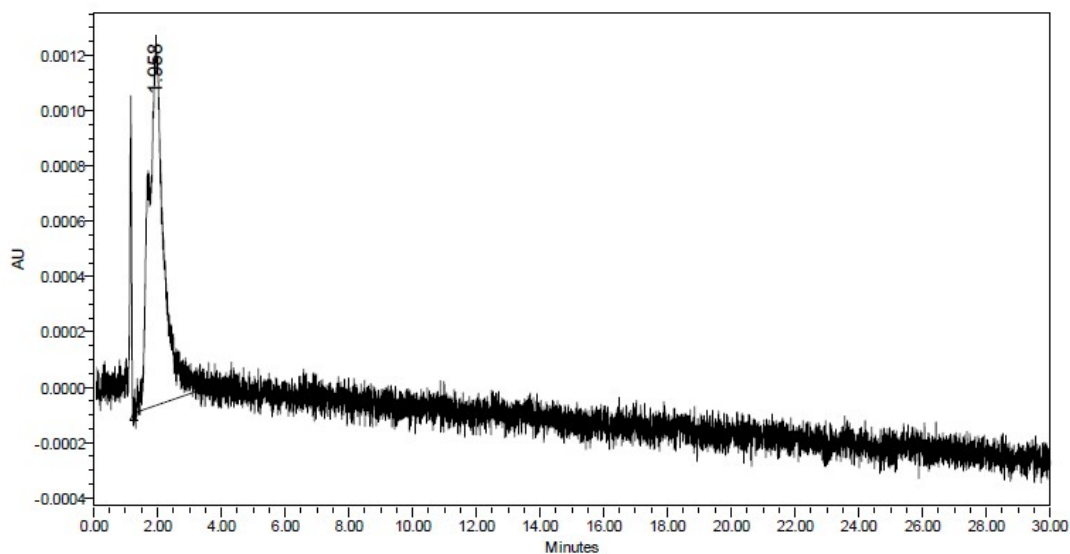
Total dye loaded = 0.1 mg

Total dye released = 0.036 mg

Loading % = [(Total drug added – Drug in the supernatant)/(Total drug added)]*100

= 64 %

SAMPLE INFORMATION			
Sample Name:	DS UN	Acquired By:	System
Sample Type:	Standard	Sample Set Name	01032022A
Vial:	2:B,7	Acq. Method Set:	JAYNI
Injection #:	1	Processing Method	JAYNI
Injection Volume:	10.00 ul	Channel Name:	490.0nm
Run Time:	30.0 Minutes	Proc. Chnl. Descr.:	PDA 490.0 nm (430-500)nm
Date Acquired:	01-Mar-22 1:12:22 PM IST		
Date Processed:	10-May-22 7:38:45 PM IST		



	RT	Area	% Area	Height
1	1.958	43762	100.00	1331

Figure S5. UPLC spectrum of DOX. The DOX was eluted isocratically at a 1 mL/min flow rate using acetonitrile: water (30:70) as eluent and detected using Waters 2998 PDA detector at the wavelength range 200-800 nm. Notably, the analysis was carried out at 490 nm, at 30 °C, using a reported method while applying some change (Thakur et al., 2019).

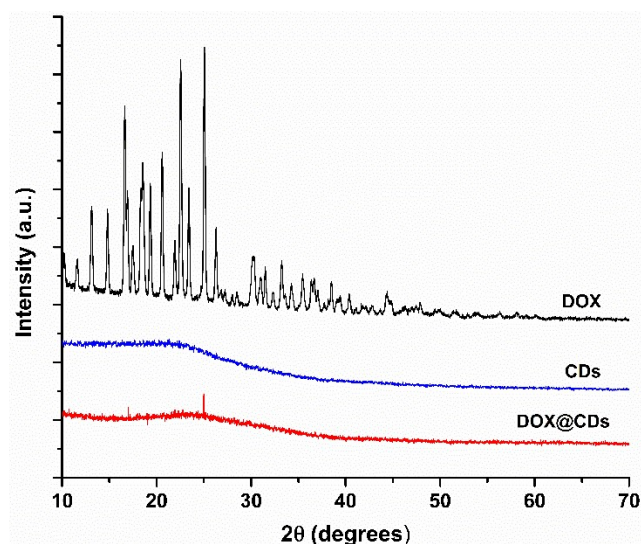


Figure S6. XRD spectra of DOX, CDs, and DOX@CDs

S6. Optimization of the Concentrations of ZnPc, PEGMA, and PAA Components Present in the Hydrogels. For the development of hydrogel, gelation time was noticed to be dependent

on the weight ratio of PEGMA: PAA: ZnPc components. Firstly, the weight ratio of PEGMA (4.28 w/v %) and ZnPc (5 mg) was kept constant and the weight % of PAA was varied from 0 to 1w/v%. By using 0 wt% PAA, the gelling process took the longest time of 30 m, and the time of gelation gradually reduced to 25, 20, and 15 m, when the weight-to-volume ratio of PAA was increased to 0, 0.5, and 1 w/v %, respectively. These results indicated that the optimum concentration of the PAA in the hydrogel improved gelation. Next, we sought to optimize the concentration of PEGMA for the development of hydrogel. For this, 0.1, 0.2, 0.3, and 0.4 g, respectively, of PEGMA were taken into consideration to optimize the hydrogel development. We noticed that 0.3 g (4.28 w/v %) of PEGMA was optimum for the development of hydrogel based on gelation time at 15 m. As shown in **figure 2a**, 0.071 w/v % (5 mg) of ZnPc transmitted 90% of laser light (0.35 mW) compared to other concentrations. The optical transmittance for hydrogel was measured with a UV–vis spectrophotometer equipped with an integrating sphere. The result illustrated the hydrogel showed maximum transmittance (90 %) at 650 nm using red laser light as shown in Figure S7.

S7. Swelling Index of the ZnPc-PP H

The water absorption ability of the developed hydrogel is advantageous to induce the anticancer treatment by absorbing effluence from the tumor microenvironment, which facilitates the hydrogel disintegration in the acidic microenvironment of the tumor. The swelling behaviors of the developed hydrogels are shown in Figure S8. The final developed hydrogel using 0.3 g PEGMA reached a maximum water absorption of upto ~ 400% of its initial weight after 72 h. On the other hand, the lowest water absorption of about 375 %, 381 %, and 387 % was observed using 0.1 g, 0.2 g, and 0.4 g of PEGMA, respectively. Hence, the swelling ratio exhibited that the optimum ratio of components in the hydrogel cross-linking improves the effectiveness of cross-linking.

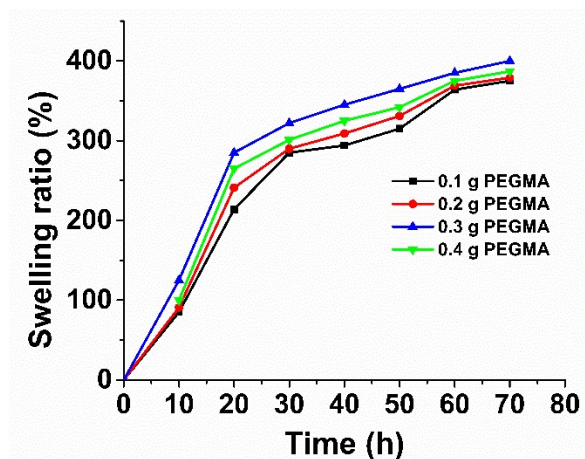


Figure S7. The swelling ratio of different concentrations of PEGMA in the developed hydrogels in PBS (pH 7.4) at 37 °C.

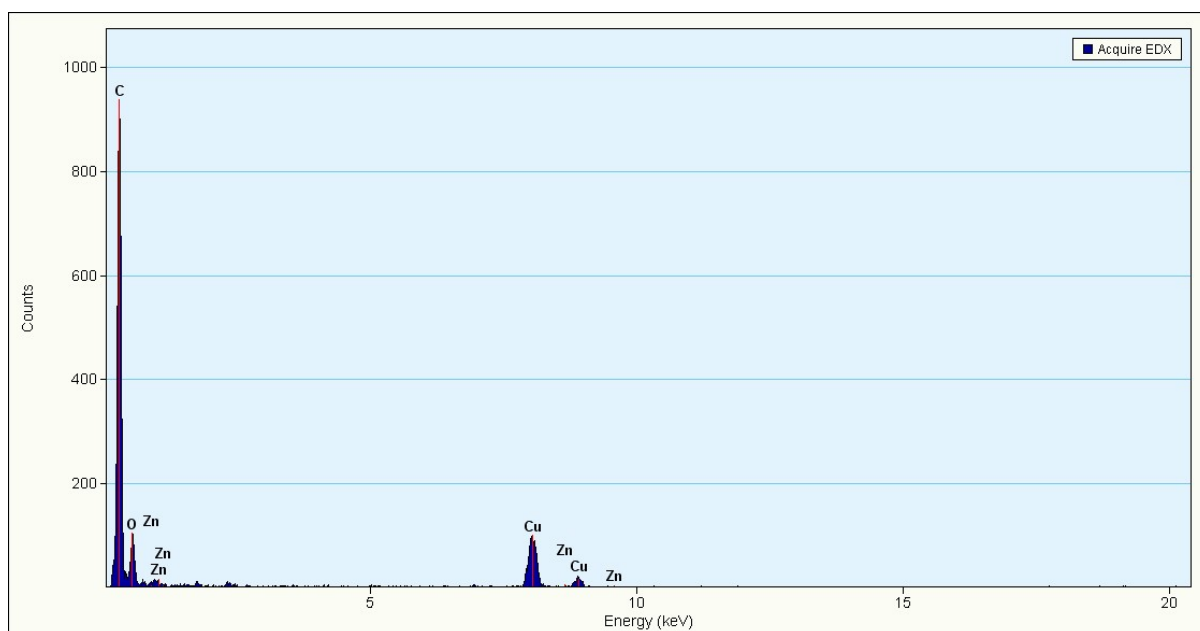


Figure S8. EDX map of ZnPc-PP H

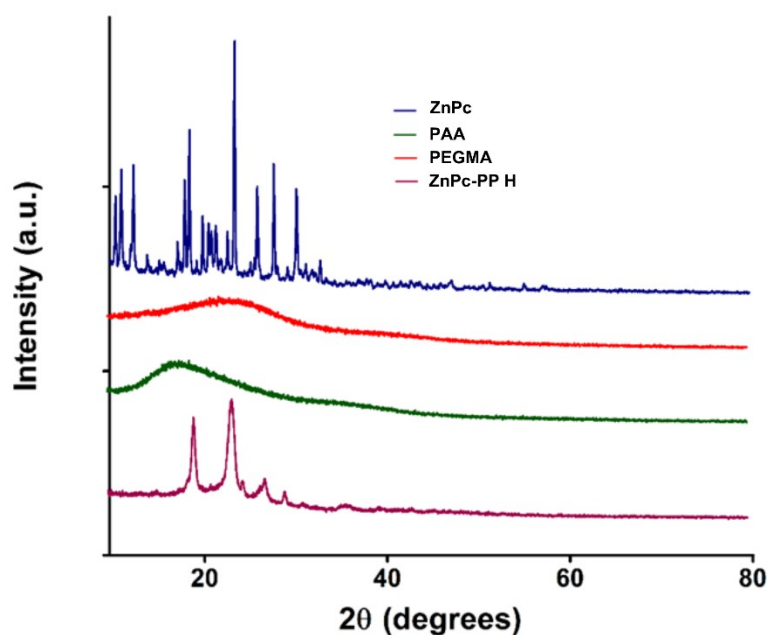


Figure S9. XRD spectra of ZnPc, PAA, PEGMA, ZnPc-PP H

S8. Brunauer-Emmett-Teller (BET) Analysis: Figure. S11a and b displayed the N_2 adsorption–desorption isotherms of ZnPc-PP H, DOX@CDs-ZnPc-PP H. Both graph profiles were representing the type IV isotherms with hysteresis loop, indicating the presence of mesopores. The BET of ZnPc-PP H is $5.964 \text{ m}^2/\text{g}$, which is higher than that of DOX@CDs-ZnPc-PP H ($8.852 \text{ m}^2/\text{g}$), indicating the presence of DOX@CDs over the surface areas of the ZnPc-PP H resulting in increased surface areas.¹ The total pore volume of ZnPc-PP H was at 0.008 cc/g and the corresponding pore size distribution determined by the Barrett–Joyner–Halenda (BJH) method was about 2.456 nm . Nevertheless, the total pore volume of DOX@CDs-ZnPc-PP H was at 0.006 cc/g , and the corresponding pore size distribution was observed at 1.230 nm , indicating that the drug was loaded successfully. **Figure S11** the presence of DOX@CDs loaded ZnPc-PP H, suggested the important role of the hydrogel as a therapeutic and drug delivery vehicle.

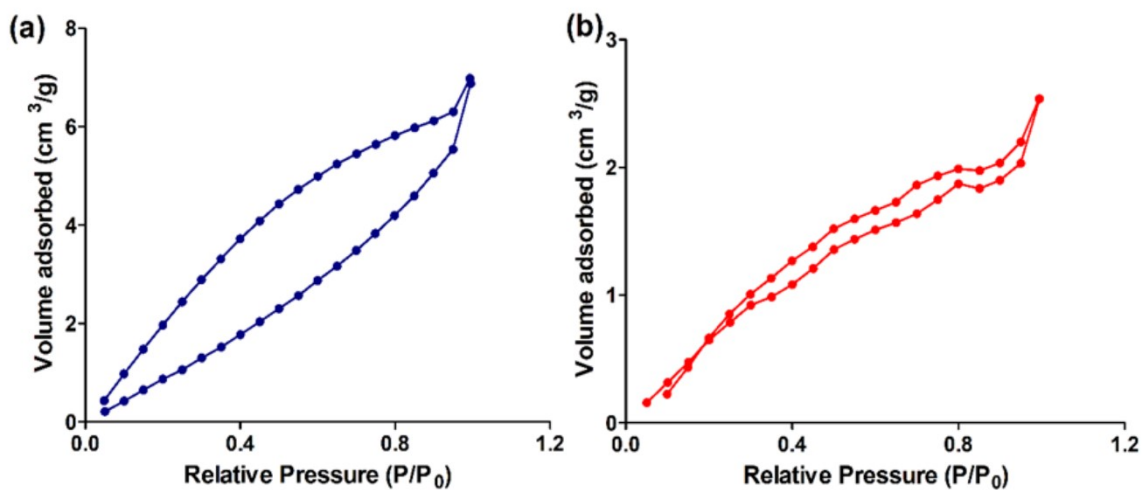


Figure S10. N_2 adsorption-desorption isotherms of ZnPc-PP H and DOX@CDs-ZnPc-PP H.

The continuous flow studies in Figures S12a and b indicated that the viscosity of Zn-PcPP H and DOX@CDs-ZnPc-PP H drops as the shear rate rises. **Figures S13a-b** also stated that the Zn-PcPP H and DOX@CDs-ZnPc-PP H have larger G' than G'' suggesting that they are shear-thinning materials

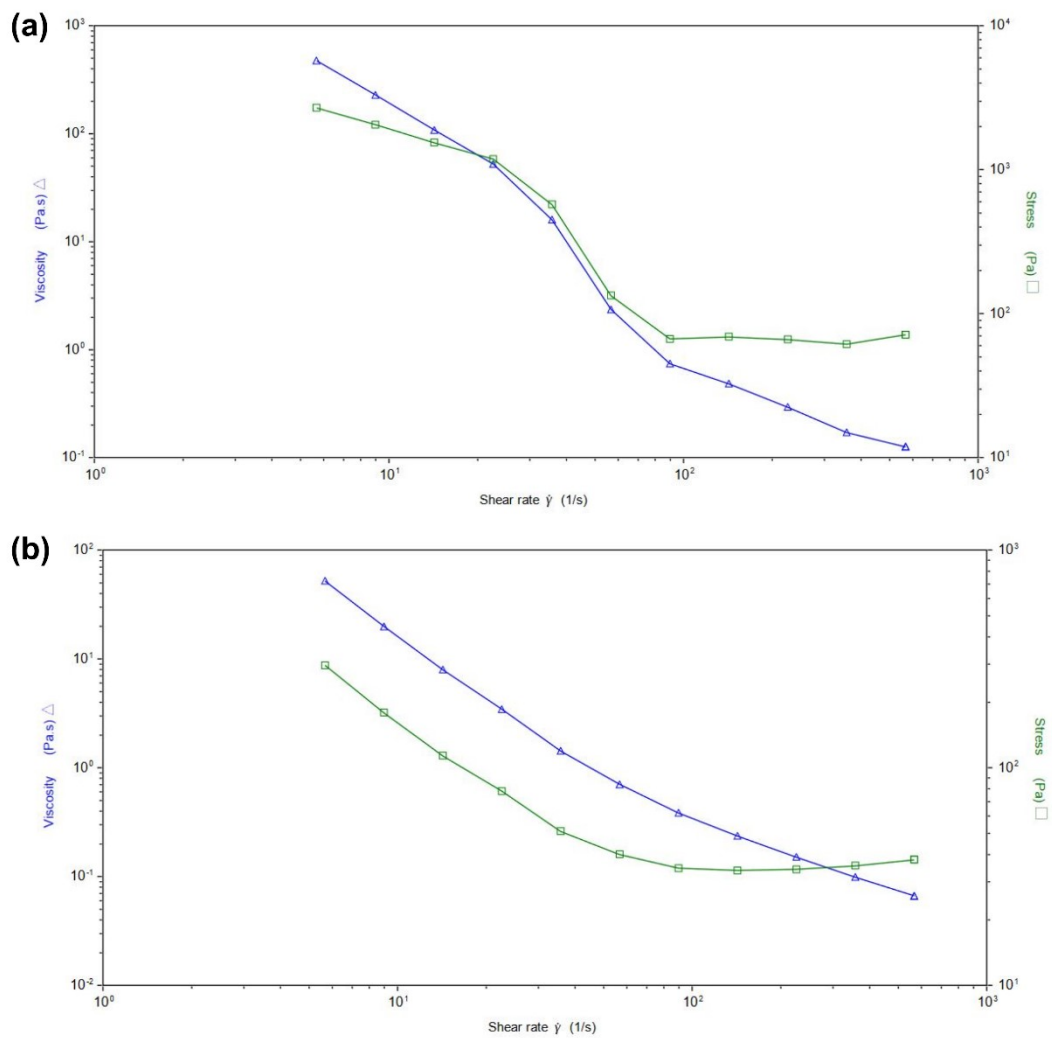


Figure S11. Rheological measurements of Zn-PcPP H and DOX@CDs-ZnPc-PP H: a) displays the viscosity vs shear rate of Zn-PcPP H and b) shows the viscosity vs shear rate of DOX@CDs-ZnPc-PP H.

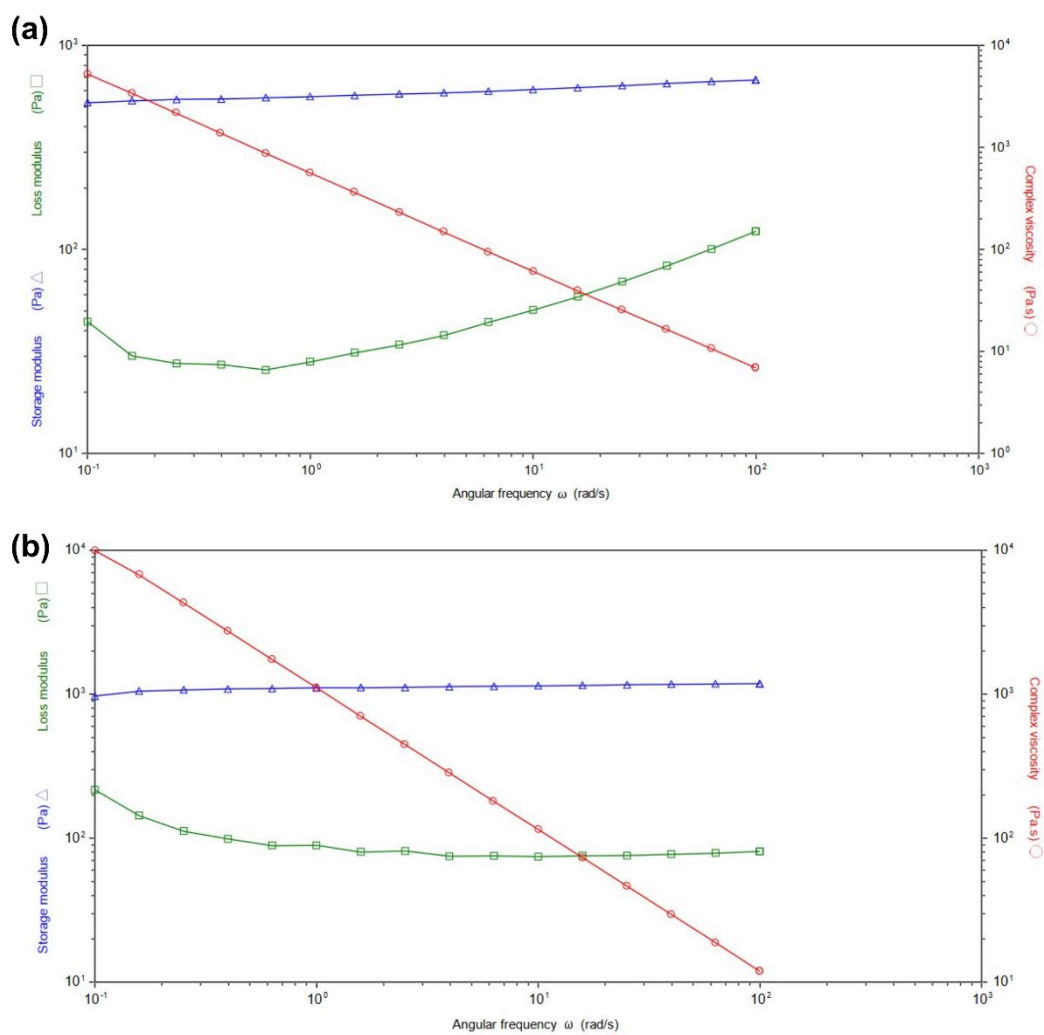


Figure S12. Rheological measurements depict the storage modulus G' and loss modulus G'' to the angular frequency of (a) Zn-PcPP H and (b) DOX@CDs-ZnPc-PP H.

Degradation of DOX@CDs-ZnPC-PP H in various pH

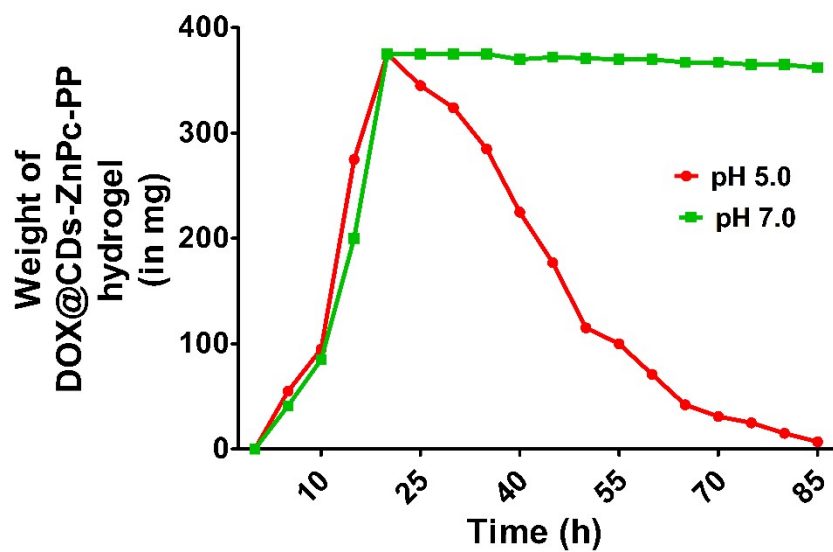


Figure S13. Degradation of DOX@CDs-ZnPC-PP H in response to various pH.

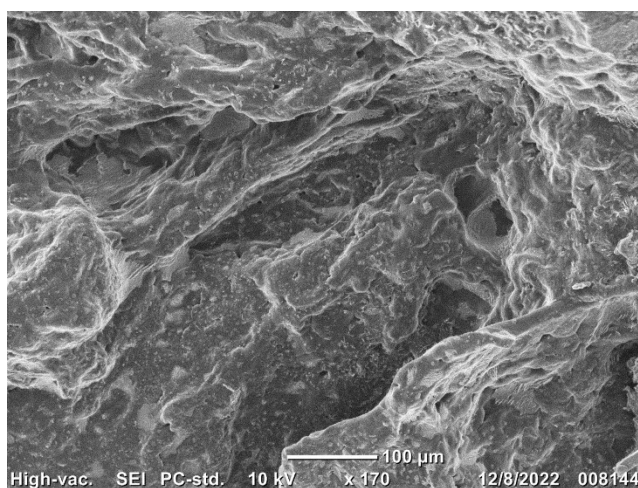


Figure S14. Scanning electron microscopy of pH-treated DOX@CDs-ZnPC-PP H.

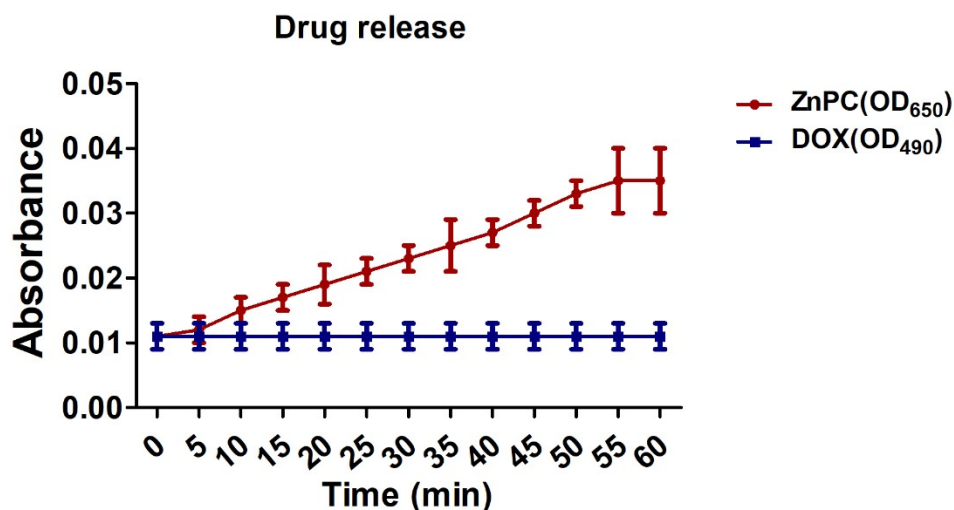


Figure S15. In vitro release of DOX and ZnPc under 650 nm laser irradiation

S9. Singlet Oxygen Quantification Assay of Synthesized Probes

Table S3. Singlet oxygen quantum yield (ϕ_{Δ}) of developed probes.

S. No	Probes	Standard equation	(ϕ_{Δ})
1	CDs	$Y = -0.4282x + 0.7387$	0.09 ± 0.001
2	DOX	$Y = -0.0137x + 0.8445$	0.20 ± 0.001
3	DOX@CDs	$Y = -0.035x + 0.821$	0.26 ± 0.002
4	ZnPc	$Y = -0.088x + 0.491$	0.98 ± 0.001
5	ZnPc-PP H	$Y = -0.089x + 1.15$	0.66 ± 0.005
6	DOX@CDs-ZnPc-PP H	$Y = -0.1162x + 1.022$	0.081 ± 0.007

S10. Optimization of laser light intensity for anticancer activity. The light intensities (namely 60 mW, 100 mW, 400 mW, and 600 mW) have been used by researchers to carry out light-induced photodynamic therapy against cancer cells.⁷ However, we assumed that the selected red laser light intensity would not trigger cell death against the MCF-7 cell lines. For this, we have optimized the different functional doses of light intensity ranges from 25 to 100 mW respectively, for 5 min of irradiation time. As shown in **figure S14**, we selected 50 mW

optimum light intensity and the cell viability percentage was 96% upon the laser light treatment.

Table S4. Optimization of the laser light intensity for MCF 7 cell treatment

S. No.	mW	cell viability (%)	Std deviation
1.	25	100	0.00
2.	30	98.50	1.92
3.	40	97.40	2.11
4.	50	96.60	3.31
5.	70	91.10	4.10
6.	90	90.63	5.27
7.	100	82.40	4.32

*Number of the experiment performed in triplicates

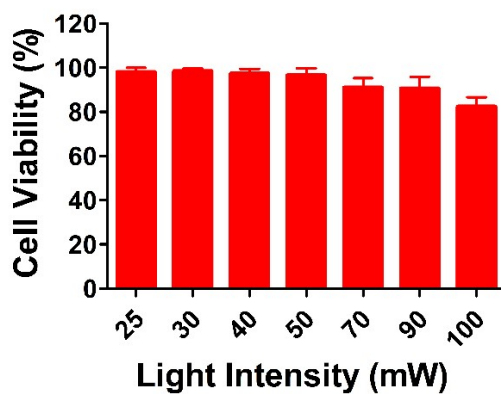


Figure S16. Effect of red laser light intensity (mW) on the viability of MCF-7 cells using 3-(4,5-dimethylthiazol-2-yl)-2,5-diphenyltetrazolium bromide (MTT) assay.

S11. Combination Index

Table S5. Combination index of at IC₅₀ values determined from the dose-dependent survival curves of free DOX and ZnPc and MCF 7 cells.

Treatment condition	Drugs Combination IC ₅₀ (µg/mL)	Concentration of drug DOX in combination IC ₅₀ (µg/mL)	Concentration of drug ZnPc in combination IC ₅₀ (µg/mL)	Combination index value
Dark	3.65	10.65	12.90	0.83
Light	1.06	10.26	3.17	0.84

S12. References

- (1) Reddy, Y. N.; De, A.; Paul, S.; Pujari, A. K.; Bhaumik, J. *In Situ* Nanoarchitectonics of a MOF Hydrogel: A Self-Adhesive and pH-Responsive Smart Platform for Phototherapeutic Delivery. *Biomacromolecules* **2023**. <https://doi.org/10.1021/acs.biomac.2c01489>.
- (2) Chandna, S.; Paul, S.; Kaur, R.; Gogde, K.; Bhaumik, J. Photodynamic Lignin Hydrogels: A Versatile Self-Healing Platform for Sustained Release of Photosensitizer Nanoconjugates. *ACS Appl. Polym. Mater.* **2022**. <https://doi.org/10.1021/acsapm.2c01319>.
- (3) Paul, S.; Thakur, N. S.; Chandna, S.; Sagar, V.; Bhaumik, J. Lignin-Based CdS Dots as Multifunctional Platforms for Sensing and Wearable Photodynamic Coatings. *ACS Appl. Nano Mater.* **2022**, 5 (2), 2748–2761. <https://doi.org/10.1021/acsanm.1c04427>.
- (4) Paul, S.; Thakur, N. S.; Chandna, S.; Reddy, Y. N.; Bhaumik, J. Development of a Light Activatable Lignin Nanosphere Based Spray Coating for Bioimaging and Antimicrobial Photodynamic Therapy. *J. Mater. Chem. B* **2021**, 9 (6), 1592–1603. <https://doi.org/10.1039/d0tb02643c>.

- (5) Bugaj, A. M. Targeted Photodynamic Therapy--a Promising Strategy of Tumor Treatment. *Photochem. Photobiol. Sci.* **2011**, *10* (7), 1097–1109. <https://doi.org/10.1039/c0pp00147c>.
- (6) Zhu, K.; Wang, C.; Liu, J.; Wang, W.; Lv, Y.; Wang, P.; Meng, A.; Li, Z. Facile Fabrication of ZnPc Sensitized G-C3N4 through Ball Milling Method toward an Enhanced Photocatalytic Property. *J. Asian Ceram. Soc.* **2020**, *8* (3), 939–947. <https://doi.org/10.1080/21870764.2020.1799912>.
- (7) Wang, X.; Kang, W.-R.; Hu, X.-M.; Li, Q. Irradiance Uniformity Optimization for a Photodynamic Therapy Treatment Device with 3D Scanner. *J. Biomed. Opt.* **2021**, *26* (07). <https://doi.org/10.1117/1.jbo.26.7.078001>.